Sturm–Liouville eigenproblems with an interior pole

John P. Boyd
Department of Atmospheric and Oceanic Science, University of Michigan, Ann Arbor, Michigan 48109

(Received 17 September 1979; accepted for publication 18 March 1981)

The eigenvalues and eigenfunctions of self-adjoint Sturm–Liouville problems with a simple pole on the *interior* of the interval $[A, B]$ are investigated. Three general theorems are proved and it is shown that as $n\to\infty$, the eigenfunctions more and more closely resemble those of an ordinary Sturm–Liouville problem and $\lambda_n \sim -m^2\pi^2/(B-A)^2$, just as if there were no singularity. The low-order modes, however, differ drastically from those of a nonsingular eigenproblem in that (i) both eigenvalues and eigenfunctions are *complex* (despite the fact the problem is self-adjoint), (ii) the real and imaginary parts of the nth eigenfunction may both have ever-increasing numbers of interior zeros as $B\to\infty$, instead of just $(n-1)$ zeros, and (iii) as $B\to\infty$, the eigenvalues for all small n may cluster about a common value in contrast to the widely separated eigenvalues of the corresponding nonsingular problem. These results are general, but in order to present quantitative solutions for the low-order modes, too, special attention is given to the particular case

$$u'' + (1/x - \lambda)u = 0, \tag{1}$$

with $u(A) = u(B) = 0$ where λ is the eigenvalue and A and B are of *opposite* signs. For small n, one can obtain the approximation

$$\lambda_n \sim \exp[(1 + 3^{1/2}i)d_n/(2B^{1/3})]/B, \tag{2}$$

where d_n is the nth root of the Airy function $\mathrm{Ai}(-z)$. The imaginary part of (2) shows explicitly how profoundly the interior pole has modified the structure of the eigenproblem.
The WKB method, which was used to derive (2), is shown to be accurate for all n. The WKB analysis is of some interest in and of itself. Although the number of WKB "transition" points is the same as for the half-century old quantum harmonic oscillator (two), the substitution of the interior pole for one of the turning points has a profound (and fascinating) impact on both the WKB formalism and the numerical results. Thus, although this problem was motivated by the physics of hydrodynamic waves, it is also an extension to both classical Sturm–Liouville theory and to the WKB treatment of eigenvalue problems.

PACS numbers: 02.30.Hq

1. INTRODUCTION

Normal self-adjoint Sturm–Liouville (SL) eigenproblems on an interval $[A, B]$ fall into two classes: those whose equations have no singularities on $[A, B]$ and those which are singular only on the boundaries. The theory of the diurnal ocean tide introduced a third class: equations which would otherwise be described by the classical SL theory except for having so-called "apparent" singularities in the interior of the domain. Although the tidal equation was derived by Laplace in the eighteenth century and despite the fact that the eigenfunctions themselves are analytic everywhere in the interior of the domain, the mathematical problems of this example of the third class were not resolved until 1970, ending a long history of confusion, controversy, and many published blunders.[1,2] The goal of the present work is to study the simplest example of a fourth class of SL eigenproblems in which the eigenfunctions themselves, as well as the differential equation, are singular in the interior of the interval.

Up to now, this fourth class of self-adjoint SL problems has been completely ignored, and small wonder. Such problems seem bizarre and outrageous: what physical theory could lead to equations whose solutions are singular inside the physical domain? In reality, such interior singularities or "critical surfaces" arise as naturally in fluid waves as kittens from cats. Physically, the singularity is removed by *friction*, which shifts it into the complex plane. In the real world, there is always at least a little friction, so the actual fluid waves are always finite and well-behaved, as one would expect. Because the dissipation is so weak, however, it is a good approximation to take the inviscid limit so as to eliminate the friction as an explicit parameter, and this will be done in most of the paper. In the next two sections, however, the friction is temporarily restored to a finite value to show how the singularity should be interpreted when making this approximation. (In brief, the conclusion is that the eigenfunctions should be made single-valued by a branch cut in the *upper* half-plane.)

Although some attention will be given to a general class of problems, for simplicity and for the sake of giving explicit results instead of vague generalizations, most of our attention will be focused on the particular example

$$u_{xx} + (1/x - \lambda)u = 0, \tag{1.1}$$

$$u(A) = u(B) = 0, \tag{1.2}$$

where λ is the eigenvalue. If A and B are of the same sign, then (1.1) and (1.2) are merely a normal, self-adjoint Sturm–

 0022-2488/81/081575-16$01.00

Liouville problem of the first kind with no singularities on $[A, B]$. Here, however, A and B will be of *opposite* signs so that both (1.1) and the eigenfunctions are singular in the interior of the interval $[A, B]$. None of the usual theorems of conventional SL theory apply because the interior singularity violates the conditions of the theorems, and most are no longer true. In particular, the eigenfunctions and eigenvalues are complex.

Thus, one has no choice but to regard (1.1) and (1.2) as a new species, a "Sturm–Liouville eigenproblem of the fourth kind," when the singularity is in the interior. The problem is not a lack of self-adjointness (it is well known that non-self-adjoint equations may have complex eigenvalues); actually, (1.1) is *self-adjoint*. The rub is solely that the differential equation has a *pole* on the *interior* of the domain.

In several years of searching, it has not been possible to locate a single paper other than this one which attempts a systematic attack on such "fourth kind" eigenproblems, but there have been three precursors. Dickinson[3] and Tung[4,5] analyzed waves with "critical latitudes" using the continuous spectrum approach discussed in Appendix B. This work is complementary to that reported here, and some of Dickinson's WKB analysis can be carried over. Simmons[6,7] is the only author besides Boyd[8] to have previously computed discrete, singular eigenfunctions, but his calculations are strictly numerical and limited to more complicated equations than (1.1).

This present work has three principal goals: (i) to prove some simple theorems about the general SL problem of the fourth kind, (ii) to obtain analytic approximations to the high- and low-order eigenvalues of (1.1) in particular, and (iii) to describe the WKB treatment of an eigenvalue problem with a turning point and a simple pole. The reasons for investigating "fourth kind" SL problems have already been explained above and also in Boyd.[8] The purpose of studying (1.1) is to understand the general class by thoroughly examining a particular example.

The WKB analysis has several motives. First, it is a straightforward and familiar method for obtaining asymptotic approximations to the solution of (1.1). In addition, however, the WKB analysis is of interest in itself. Generations of budding physicists have studied the quantum mechanical harmonic oscillator from a WKB viewpoint. Here, however, although the number of WKB "transition points" is the same (two), the replacement of a turning point by a simple pole profoundly alters the solution, and it is fascinating to see how the application of such familiar ideas can lead to such radically different conclusions.

The plan of the paper is as follows. The next section proves three theorems for general Sturm–Liouville problems of the fourth kind. Section 3 gives the exact analytic solution of (1.1) in terms of Whittaker functions and also the rather unorthodox choice of branch cut which is physically appropriate for making the eigenfunctions single-valued. The next two sections discuss the eigenvalues and eigenfunctions in the limits $n\to\infty$ and $n\to 0$, respectively. Sections 6 and 7 analyze the WKB method and its accuracy. The eighth section is a case study of the complete spectrum for a particular choice of parameters, paying particular attention to modes of intermediate n. The final section summarizes the similarities and differences between normal Sturm–Liouville eigenproblems and those of the singular fourth kind discussed here. The three appendices discuss the Whittaker functions, discrete versus continuous eigenvalues, and Chebyshev approximations for the eigenvalues, respectively.

The theorems of Sec. 2 and the asymptotic $n\to\infty$ approximations of Sec. 4 [Eqs. (4.6) and (4.10)] are applicable to general Sturm–Liouville eigenproblems of the fourth kind. Most of the remaining results are quantitatively applicable only to the particular example (1.1), but the methods used to derive them are general also.

2. THREE THEOREMS

In this section, some simple results will be proved for an equation more general than (1.1). To interpret the singularity of (2.1), the friction ϵ is explicitly included. As noted in the introduction, ϵ is normally so small that it is good approximation to take the limit $\epsilon\to 0$, which reduces the number of parameters from three (ϵ, A, B) to two (A and B).

Theorems

Let $u_m(x)$ and $u_n(x)$ be eigenfunctions of the differential equation

$$u_{xx} + [r(x)/(x - i\epsilon) + p(x) - \lambda\,]u = 0, \tag{2.1}$$

with

$$u(A) = u(B), \tag{2.2}$$

where $p(x)$ and $r(x)$ are real and analytic on $[A, B]$, λ is the eigenvalue, A and B are of opposite signs, and $\epsilon > 0$ is a real constant. Then in the limit $\epsilon\to 0$, one can prove

Theorem 1: If $\lambda_m \neq \lambda_n$, the eigenfunctions are *orthogonal*, i. e.,

$$\int_A^B u_m u_n\, dx = 0. \tag{2.3}$$

Theorem 2: Letting $\mathrm{Im}(\lambda_n)$ denote the imaginary part of the eigenvalue,

$$\mathrm{Im}(\lambda_n)\int_A^B |u_n|\, dx = \pi |u_n(0)|^2 r(0). \tag{2.4}$$

Theorem 3: The eigenvalue λ is always in the upper half-plane, i. e.,

$$\mathrm{Im}(\lambda_n) \geqslant 0 \quad \text{for all } n, \tag{2.5}$$

if $r(x) > 0$.

Proofs

The demonstration of Theorem 1 is identical with the proof of orthogonality for orthodox Sturm–Liouville problems as given in Morse and Feshbach,[2] for example. Let

$$q(x) \equiv r(x)/(x - i\epsilon) + p(x). \tag{2.6}$$

Writing the differential equations satisfied by $u_m(x)$ and $u_n(x)$ after multiplication by the other mode gives (letting primes denote differentiation)

$$u_m(u_n'' + qu_n - \lambda_n u_n) = 0, \tag{2.7}$$

$$u_n(u_m'' + qu_m - \lambda_m u_m) = 0. \tag{2.8}$$

Subtracting (2.8) from (2.7) gives

$$u_m u_n'' - u_n u_m'' + (\lambda_m - \lambda_n) u_m u_n = 0. \tag{2.9}$$

The offending singular term $q(x)$ has already disappeared through subtraction, and the remaining steps—rewriting the first two terms in (2.9) as a perfect derivative, integrating from A to B, and invoking the homogeneous boundary conditions—give

$$(\lambda_m - \lambda_n) \int_A^B u_m(x) u_n(x)\, dx = 0, \tag{2.10}$$

from which (2.3) is obvious.

The steps in the proof of the second theorem are formally identical to those for the first except that $u_m(x)$ is replaced by $u_n(x)^*$ where the asterisk denotes the complex conjugate. Since $u_n(x)$ cannot be orthogonal to its own complex conjugate, this argument is used in formal Sturm–Liouville theory to show that $\lambda_n^* = \lambda_n$, i. e., all the eigenvalues are real. For the singular class examined here, the rub is that because of the pole (and the friction ϵ), $q(x) \neq q(x)^*$, so the singular terms do *not* cancel out and the equivalent of (2.9) is

$$u_n u_n^{*''} - u_n^* u_n'' + (\lambda_n - \lambda_n^*) |u_n|^2 = (q - q^*) |u_n|^2. \tag{2.11}$$

Following through the remaining steps gives

$$(\lambda_n - \lambda_n^*) \int_A^B |u_n|^2\, dx = \int_A^B \frac{|u_n|^2 2i\epsilon r(x)}{x^2 + \epsilon^2}\, dx. \tag{2.12}$$

Carrier, Krook, and Pearson[9] show that

$$\lim_{\epsilon \to 0} \frac{\epsilon}{x^2 + \epsilon^2} = \pi \delta(x). \tag{2.13}$$

Substituting this into (2.12) and performing the integration on the right-hand side gives (2.4).

The third theorem follows trivially from the second. Since all the other quantities in (2.4) are absolute values and therefore positive semidefinite, it follows that $\mathrm{Im}(\lambda_n)$ must be as well.

A few remarks are in order. First, only Theorem 2 actually requires $\epsilon \to 0$; the third theorem can be proved directly from (2.12).

Second, Theorem 1 shows that the eigenfunctions are mutually orthogonal among themselves. The orthogonality relation (2.3) does not involve the complex conjugates of the eigenfunctions nor is (2.3) a biorthogonality equation involving inner products of the eigenfunctions paired with those of the adjoint. Despite its complex eigenvalues, (1.1) with (1.2) is *self-adjoint* and the form of the orthogonality relation, Theorem 1, reflects this.

The second theorem shows that $\mathrm{Im}(\lambda_n) = 0$ only when

$$u_n(0) = 0, \tag{2.14}$$

i. e., in the very special case that $u_n(x)$ is nonsingular. When $p(x) = 0$ this means $u_n(x)$ is proportional to $M_{-\kappa, \frac{1}{2}}(-x/\kappa)$, which always has a zero at $x = 0$. Since (2.14) plus (2.2) are equivalent to imposing *three* boundary conditions on a *second* order differential equation, Theorem 2 implies that λ_n is *real* on a set of *measure zero*. In other words, there are certain sets of values of (A, B, n) for which λ_n is real, but if one chooses A and B at random, the odds are infinitesimally small that any of the modes will have a real eigenvalue (although the imaginary parts of some may be very small).

Theorem 3 states what will be assumed in later sections in working out the WKB formalism: that λ is always in the upper half-plane and κ [defined by (3.4) below] therefore, always in the fourth quadrant. The physical significance (and necessity!) of this are discussed in Boyd.[8] The condition that $r(x)$ be positive is equivalent to satisfying the well-known Rayleigh–Kuo criterion for barotropic stability, and is almost always true in the upper atmosphere. It is automatically satisfied by the linear wind shear model [$r(x) = \mathrm{const}$] that will be considered in the rest of this paper.

3. THE EXACT SOLUTION OF THE MODEL PROBLEM

The general problem

$$u_{zz} + (\alpha/z - \lambda')u = 0, \tag{3.1}$$

$$u(A') = u(B') = 0, \tag{3.2}$$

can be reduced to the canonical form (1.1) and (1.2) through the substitutions

$$x = \alpha z, \tag{3.3a}$$

$$A = \alpha A', \tag{3.3b}$$

$$B = \alpha B', \tag{3.3c}$$

$$\lambda = \lambda'/\alpha^2. \tag{3.3d}$$

Equation (1.1) is a special case of Whittaker's equation, which in turn is merely a transformed version of the confluent hypergeometric equation. Defining (principal branch)

$$\kappa \equiv 1/2\lambda^{1/2}, \tag{3.4}$$

the linearly independent solutions may be taken as

$$u_1(x, \lambda) = M_{-\kappa, \frac{1}{2}}(-x/\kappa), \tag{3.5}$$

$$u_2(x, \lambda) = \Gamma(1 + \kappa) W_{-\kappa, \frac{1}{2}}(-x/\kappa). \tag{3.6}$$

The power series for these Whittaker functions and their relations to the usual M and U confluent hypergeometric functions are given in Appendix A. The minus signs in (3.5) and (3.6) are a convention introduced by Dickinson to ensure that the Whittaker functions have different asymptotic be-

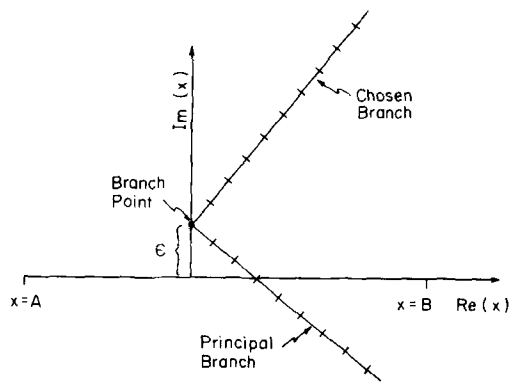

FIG. 1. Two possible branch cuts for the solution of Eq. (2.7) with friction coefficient ϵ and complex eigenvalue λ. The principal branch of the Whittaker function cuts the real axis between the boundaries A and B, which would make the solution discontinuous. The chosen branch is convenient and avoids this discontinuity. Any other branch cut which avoids the real axis would be acceptable, however.

havior ($M_{-\kappa,\frac{1}{2}}$ blows up and $W_{-\kappa,\frac{1}{2}}$ decays) as $x\to-\infty$. With this convention, the lowest few eigenfunctions are approximately proportional to the W function alone, as explained in the next section, which is a great simplification.

$M_{-\kappa,\frac{1}{2}}(y)$ is an entire function, but $W_{-\kappa,\frac{1}{2}}(y)$ has a branch point at $y=0$. The obvious choice is to take the principal branch of the function, but this is not physically allowed. If one inserts a small amount of dissipation with friction coefficient ϵ (with the understanding that $\epsilon\to 0$ in the end), (1.1) becomes

$$u_{xx}+[1/(x-i\epsilon)-\lambda]u=0, \tag{3.7}$$

and the singularity is shifted into the upper half-plane. If one uses the fact that κ lies always in the fourth quadrant (proved in Sec. 2), then the branch cut for the principal branch of $W_{-\kappa,\frac{1}{2}}(-x/\kappa)$ would cross the real x axis as shown schematically in Fig. 1, which is absurd. The simplest allowable choice is to place the branch cut along the ray

$$\arg y=-\pi/2, \tag{3.8}$$

where (note the sign difference between y and x)

$$y\equiv -x/\kappa. \tag{3.9}$$

Dickinson[3] made the same choice. Any branch cut which lies above the real x axis is permitted, however, and in fact the different choice $\arg x=\pi/2$ is made in Fig. 5 for the sake of clarity. Since there is always (weak) damping in a real fluid, such frictional arguments have been used to choose the proper branch in fluid mechanics for a very long time.

Unfortunately, this nonstandard choice of branch implies that the usual textbook asymptotic formulas for $W_{-\kappa,\frac{1}{2}}(y)$ cannot be directly applied to our Whittaker function when y is in the third quadrant. However, it is a property of logarithmic solutions to linear, second-order differential equations that the coefficient of the logarithm is always proportional to that solution of the equation—in this case, $M_{-\kappa,\frac{1}{2}}(y)$—which is analytic at $y=0$. If one defines $\ln(y)$ to be the logarithm with branch cut at $\arg y=-\pi/2$ and $\ln^{(P)}(y)$ to be the principal branch of the logarithm, then

$$\ln(y)=\begin{cases}\ln^{(P)}(y), & -\pi/2\leqslant\arg y\leqslant\pi\\ \ln^{(P)}(y)+2\pi i, & \pi<\arg y\leqslant 3\pi/2\end{cases}. \tag{3.10}$$

From this it follows that

$$W_{-\kappa,\frac{1}{2}}(y)=\begin{cases}W^{(P)}_{-\kappa,\frac{1}{2}}(y), & -\pi/2\leqslant\arg y\leqslant\pi\\ W^{(P)}_{-\kappa,\frac{1}{2}}(y)+\dfrac{2\pi i\kappa}{\Gamma(1+\kappa)}M_{-\kappa,\frac{1}{2}}(y), & \pi<\arg y\leqslant 3\pi/2\end{cases}. \tag{3.11}$$

The most efficient way to evaluate the Whittaker functions is by numerical integration of (1.1), using the power series for $M_{-\kappa,\frac{1}{2}}(y)$ and $W_{-\kappa,\frac{1}{2}}(y)$ to initialize the calculation for small y. Even though (1.1) is "stiff" in the parlance of numerical analysis, an ordinary fourth-order Runge–Kutta program gave high accuracy even for large x, and was used to compute the "exact" results presented in later sections.

Letting

$$u(x,\lambda)=\alpha u_1(x,\lambda)+\beta u_2(x,\lambda), \tag{3.12}$$

the boundary conditions (1.2) can be written in the form of a 2×2 matrix equation whose determinant is

$$\Delta(x,\lambda)=u_1(A,\lambda)u_2(B,\lambda)-u_1(B,\lambda)u_2(A,\lambda). \tag{3.13}$$

The eigenrelation is then

$$\Delta(\lambda)=0. \tag{3.14}$$

Once the eigenvalues have been determined from (3.14), it is trivial to solve the matrix equation for α and β in (3.12) to obtain the eigenfunctions.

4. HIGH-ORDER MODES

In the limit $|y|\to\infty$ with κ fixed, the Whittaker functions have the familiar asymptotic approximations

$$M_{-\kappa,\frac{1}{2}}(y)=S[\sin(\kappa\pi)/\kappa\pi]\Gamma(1+\kappa)W^{(P)}_{-\kappa,\frac{1}{2}}(y)+\frac{e^{y/2}y^{\kappa}}{\Gamma(1+\kappa)}\left(1-\frac{\kappa(1-\kappa)}{y}-\frac{\kappa(1-\kappa)(1-\kappa)(2-\kappa)}{y^2}+\cdots\right), \tag{4.1}$$

$$\Gamma(1+\kappa)W^{(P)}_{-\kappa,\frac{1}{2}}(y)=\frac{\Gamma(1+\kappa)e^{-y/2}}{y^{\kappa}}\left(1-\frac{\kappa(1+\kappa)}{y}+\frac{\kappa(1+\kappa)(1+\kappa)(2+\kappa)}{y^2}-\cdots\right), \tag{4.2}$$

where

$$S=\begin{cases}-e^{i\pi\kappa} & \mathrm{Im}(y)>0,\\ -e^{-i\pi\kappa} & \mathrm{Im}(y)<0,\end{cases} \tag{4.3}$$

and where the superscript (P) denotes the principal branch of the Whittaker function as before. The asymptotic approximation to our Whittaker function of unorthodox branch can be obtained from (4.1) and (4.2) via (3.11).

In the limit $\lambda\to\infty$, $\kappa\to 0$ along the negative imaginary axis, and (4.1) and (4.2) simplify to

$$M_{-\kappa,\frac{1}{2}}(-x/\kappa)\approx -2i\sin(|\lambda|^{\frac{1}{2}}x), \tag{4.4}$$

$$\Gamma(1+\kappa)W_{-\kappa,\frac{1}{2}}(-x/\kappa)\approx e^{i|\lambda|^{1/2}x}, \tag{4.5}$$

for fixed x (at either sign) with relative error $O(1/4\lambda x)$ where the Whittaker function has a branch cut at $\arg y = -\pi/2$. Substituting (4.4) and (4.5) into (3.14) gives

$$\lambda_n = -\pi^2 m^2/(B-A)^2, \quad n \to \infty. \tag{4.6}$$

Several features of this eigenrelation deserve comment.

First, the integer m that appears in (4.6) is not necessarily equal to the mode number n when the modes are ordered according to $|\lambda|$. A counterexample where $m = n + 2$ is given in Table IV of Sec. 8.

Second, (4.6) implies that as was assumed in obtaining it, $\lambda_n \to -\infty$ as $n \to \infty$. Thus, the derivation of (4.4) through (4.6) is consistent.

Third, if we generalize (1.1) to

$$u_{xx} + [1/x - \lambda + p(x)]u = 0, \tag{4.7}$$

as done in the theorems of Sec. 2, where $p(x)$ is analytic on $[A,B]$, then

$$p(x) \ll \lambda \tag{4.8}$$

uniformly on $[A,B]$ in the limit that λ is large. Thus, the function $p(x)$ is only a small perturbation to the eigenmodes of (1.1) for sufficiently large n. Therefore, (4.6) is a valid approximation to the large eigenvalues of (4.7) for *general* bounded $p(x)$—though of course the approximation is more accurate (for a given n) when $p(x) = 0$ than when it is nonzero. One could presumably correct for $p(x) \neq 0$ along the lines of the usual Rayleigh–Schrödinger perturbation theory, but (4.6) will suffice for the present.

Fourth, (4.6) is identical with the eigenrelation of the same problem with the *pole removed*, i. e.,

$$u_{xx} - \lambda u = 0, \tag{4.9}$$

with the usual boundary conditions (1.2). Further, the eigenfunctions of (4.9) are given by a linear combination of the trigonometric eigenfunctions of (4.4) and (4.5),

$$u_n(x) \sim \sin(m\pi x/[B-A]). \tag{4.10}$$

Thus, for the *high n* modes of an equation with an interior pole, the singularity is essentially irrelevant. The solutions differ from those of (4.9) only in two small ways.

First, λ_n always has a small imaginary part λ_{im} which appears to decrease roughly as $O(1/n)$.[10] Second, the approximation (4.10) breaks down in an internal boundary layer of width $O(1/\lambda)$ about the singularity at $x = 0$, where the full Whittaker functions must be used. Since both λ_{im} and the width of the internal boundary layer decrease as $n \to \infty$, however, it still remains true that the singularity has little effect on the higher-order modes.

5. LOW-ORDER MODES

When λ is small, the internal boundary layer in which the asymptotic series (4.1) and (4.2) are inaccurate includes the whole of $[A,B]$, and more powerful, (and alas, more complicated) methods are needed. There is, however, one powerful simplification that we can make before applying them.

When n is large, λ hugs the negative real axis and the eigenfunctions are sinusoidal as shown explicitly by (4.4) and (4.5). For the low-order modes, however, λ is complex with either a large imaginary part or a positive real part; and then the eigenfunction must decay exponentially on $[A,0]$ away from the pole.

The reason for this decay is most easily seen by assuming λ is real and positive (as it is in the limiting case) and looking at the equation to which (1.1) reduces for large $|x|$:

$$u_{xx} - \lambda u = 0. \tag{5.1}$$

In order to satisfy the boundary condition of vanishing at $x = A$ where A is negative, $u(x)$ must be of the form

$$u = (\text{const})(e^{-\lambda^{1/2}|x|} - e^{-2\lambda^{1/2}|A|} e^{\lambda^{1/2}|x|}), \tag{5.2}$$

which is approximately

$$u(x) \simeq (\text{const}) e^{-\lambda^{1/2}|x|} \tag{5.3}$$

everywhere on $[A,B]$ except in a narrow boundary layer of width $O(1/\lambda^{\frac{1}{2}})$ near $x = A$ where the growing exponential is significant. In this boundary layer, however, $u(x)$ is exponentially small in comparison to its value at $x = 0$ (by a factor of $e^{-\lambda^{1/2}|A|}$), so the *absolute* error in replacing the exact solution (5.2) by the approximation (5.3) is exponentially small *everywhere* on $[A,B]$.

In general, of course λ is complex rather than real and we want to solve (1.1) rather than (5.1), but these complications do not affect the basic argument in the least. The sign of $1/x$, like that of $-\lambda$, is negative for $x < 0$, so the pole merely makes the two linearly independent solutions grow or decay faster. The complexity of λ will cause *oscillatory* growth or decay, but the growth or decay is still there unless λ is negative real—as is approximately true for the high order modes discussed in the previous section.

Thus, the qualitative behavior of the solutions of (5.1) is identical with that of the low order eigenfunctions of (1.1). From the asymptotic approximations (4.1) and (4.2), one sees that $M_{-\kappa,\frac{1}{2}}(-x/\kappa)$ is analogous to the positive exponential in (5.2) while $W_{-\kappa,\frac{1}{2}}(-x/\kappa)$ decays exponentially away from the pole. (These asymptotic approximations may not be *numerically* accurate for the small λ we are interested in here, but they do indicate the correct exponential growth-/decay behavior as one can verify from the more powerful WKB approximations of the next section). Thus, it must be approximately true, in analogue to (5.3), that

$$u(x) \sim W_{-\kappa,\frac{1}{2}}(-x/\kappa) \tag{5.4}$$

—in words, that the low order eigenfunction is proportional to the W-function alone.

This approximation, which is equivalent to setting

$$A = -\infty \tag{5.5}$$

since (5.3) and (5.4) are exact in this limit, is justified provided

$$e^{-2\lambda^{1/2}A} \ll 1. \tag{5.6}$$

In the next section, we will assume (5.5) and then check *a posteriori* that (5.6) is in fact satisfied for small n and not-too-small A and B.

This assumption (5.5) and the reasoning behind it is important both physically and mathematically. Physically, the argument is important because it tells us that the low-order eigenfunction has nothing except an exponentially decaying tail to the left of $x = 0$—in startling contrast to the high n

modes, which are oscillatory on *both* sides of $x = 0$. Figure 2 compares the amplitudes for a typical low-order and a typical high-order mode. (To avoid repeating "small n modes" and "large n modes" *ad nauseam*, it is convenient to introduce the terms "monokeric,"—literally, "one-sided"—for a model which has only an exponentially decaying tail to the left of $x = 0$ as in the top of Fig. 2, and "dikeric"—"two-sided"—for a mode which is sinusoidal on both sides of $x = 0$ as in the bottom of Fig. 2.) Mathematically (5.5) is significant because it reduces the number of parameters from two (A and B) down to one (B alone).

Turning to the eigenvalues, we show in the next section that for small n and moderate or large A and B, i. e., a "monokeric" small λ mode

$$\lambda_n \sim (1/B)\exp[(1 + 3^{1/2}i)|d_n|/(2B^{1/3})], \tag{5.7}$$

where

$$d_n = |\tfrac{3}{8}\pi(4n - 1)|^{2/3} \tag{5.8}$$

is the nth root of Airy's function Ai$(-x)$. The hodograph of the product of B with the exact λ_1 (as determined by numerical integration) in the complex plane is shown in Fig. 3. The approximation (5.7) is a good qualitative description of the entire graph.

As $B \to \infty$, (5.7) becomes exact and

$$\lambda_n \sim 1/B \tag{5.9}$$

independently of n. This clustering of eigenvalues for large B is in sharp contrast to ordinary SL theory, where for the boundary conditions (1.2), one can prove that the eigenvalues must always be distinct and well-separated.

For finite B, (5.7) and the hodograph show that the eigenvalue is complex even though the differential equation (1.1) is both real and self-adjoint. This again would be provably impossible for a real, self-adjoint Sturm–Liouville problem of the usual classes.

The hodograph of λ is shown only for the lowest mode because one can prove from (5.7) that

$$\lambda_n(B) = \frac{9}{(4n-1)^2}\lambda_1\left[\frac{9B}{(4n-1)^2}\right]. \tag{5.10}$$

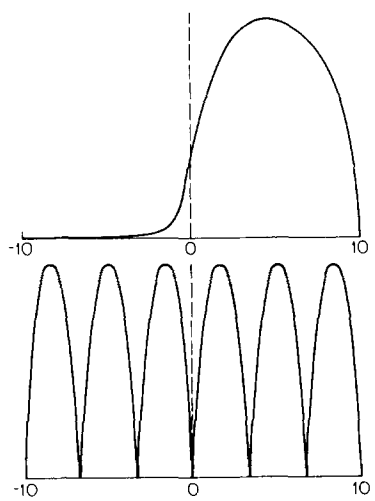

FIG. 2. A comparison of the absolute value of a low order, small $|\lambda|$, monokeric mode with that of a high order, large $|\lambda|$, dikeric mode.

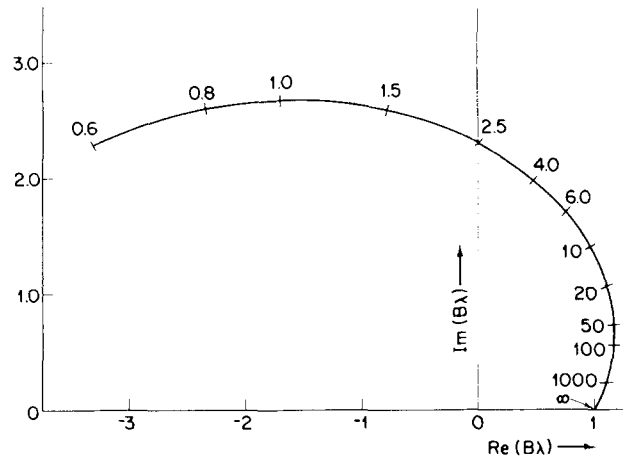

FIG. 3. The hodograph in the complex plane of the lowest eigenvalue for $A = -\infty$. The numbers labelling the curve give the values of B. Note that $B\lambda$, rather than λ itself, is the quantity plotted.

Thus, to within the accuracy of (5.7), the hodograph for λ_1 will apply to all the low-order modes with appropriate rescaling of the axes and tic-marks.

As $B \to 0$, or equivalently as $n \to \infty$ for fixed B, one can see from Fig. 2 that λ is tending towards the negative imaginary axis. This, of course, is what has been already been shown by (4.6). Thus, the high n and low n modes blend smoothly into one another.

For intermediate values of n neither (4.6) nor (5.7) is a good approximation, and the eigenfunctions are hybrids of the two extreme forms shown in Fig. 2. Nonetheless, enough has been obtained to give a good qualitative picture of the whole spectrum. In the next section, we will explore the bizarre behavior of the low-order modes via WKB, derive (5.7), and discuss its accuracy.

6. WKB

A. The method of matched asymptotic expansions

The grand strategy of this section is to derive asymptotic approximations by combining the WKB method with the method of matched asymptotic expansions (MMAE).

Although the WKB method itself is of ancient lineage, this pairing with the MMAE technique has been widely used only in the last decade. Historically, the WKB "connection formulas" were derived through a variety of coordinate transformations, integral representations, and other arguments. The books by Heading,[11] Dingle,[12] and Olver[13] describe this line of WKB development and extensions to higher order. After the MMAE method had been developed to a high art for boundary layer problems in fluid mechanics, however, it was recognized that it could be applied to a huge variety of other problems including WKB. The recent books by Bender and Orszag[14] and Nayfeh[15] present this "revisionist" derivation of WKB as well as a thorough treatment of the method of matched asymptotic expansions and its many uses. Because of its versatility and its familiarity to fluid dynamicists the WKB/MMAE approach is adopted here.

B. "Transition" points

Over most of the complex plane, Dickinson[3] showed that the WKB approximation to the general solution of (1.1) is given by an arbitrary linear combination of $W_-(x)$ and $W_+(x)$, where

$$W_-(x) = -iQ(x)^{-1/4}\exp[-2\kappa i\phi(\lambda x) + i\pi/4], \quad (6.1)$$

$$W_+(x) = Q^{-1/4}(x)\exp[2\kappa i\phi(\lambda x) - i\pi/4], \quad (6.2)$$

where, as defined in (3.4), $\kappa = \frac{1}{2}\lambda^{-1/2}$ and

$$Q(x) = 1/x - \lambda, \quad (6.3)$$

$$\phi(y) = \int_0^y \left(\frac{1}{x} - 1\right)^{1/2} dx \quad (6.4)$$

$$= \sin^{-1}y^{1/2} + y^{1/2}(1-y)^{1/2}. \quad (6.5)$$

The exceptional regions are the neighborhoods of the "transition points," which are defined to be the points where $Q(x)$ is either 0 or ∞—both make the WKB approximation singular.

The transition points thus play a central role in the analysis. Indeed, one can classify WKB problems according to the number and type of transition points in the same spirit in which one can classify a linear differential equation according to the number and type of its singularities.

The Whittaker equation (1.1) has two transition points: a simple pole at $x = 0$ and a "turning point" at

$$x_t = 1/\lambda. \quad (6.6)$$

The quantum harmonic oscillator, which is used as an example by most physics texts also has two transition points, but both are turning points.

In the parlance of matched asymptotics, the neighborhoods of the transition points constitute internal boundary layers. The WKB approximation using (6.1) and (6.2) is the "outer" solution; in the "inner" regions surrounding the transition points, $u(x)$ must be approximated using transcendentals more complicated than the exponentials appearing in (6.1) and (6.2). By matching the inner and outer solutions together and using the boundary conditions, one obtains a complete approximation to the problem.

When the differential equation has two transition points, however, there are two ways to carry out this recipe. The first is to define the inner region so that it simultaneously encloses *both* transition points. In this case, the inner approximation involves a sum of Whittaker functions (one turning point and one pole) or parabolic cylinder functions (two turning points), since these are the simplest functions with the required number of transition points. This would seem to send us round in circles when we attempt to solve (1.1) itself, but to apply asymptotic matching to fully determine the outer (WKB) solution of (1.1) and the eigenvalue, we need only the asymptotic expansions of the Whittaker functions given by (4.1) and (4.2) above, not the Whittaker functions themselves. Requiring that the WKB (outer) solution vanish at $x = B$ (and at $A = -\infty$) then gives the eigenrelation (7.1) below.

The alternative is to define two separate inner regions, one around each transition point. In this case, the inner solutions both involve Bessel functions of different orders—order one near the pole and order one-third (Airy functions) near the turning point. Though seemingly more complicated than the jointly matched or "Whittaker" matching described above, this separate or "double Bessel" matching has powerful advantages. First, because Bessel functions are simpler transcendentals than Whittaker functions, the double-inner-region method gives a simpler eigenrelation (7.1 is a function of two parameters, 7.4 only of one). Second, the use of separate inner approximations permits deeper and more precise insight into $u(x)$ instead of lumping both near-the-pole and near-the-turning point behavior together and hiding them behind the mysterious, inscrutable veil of a Whittaker function. Consequently, it is upon this "double Bessel" matching that our discussion will center.

Since the local analysis and the matching of inner and outer solutions has already been done—for the pole, by Dickinson,[3] and for the turning point by a number of independent workers more than a half a century ago—we shall merely quote their results. The challenge is to fit these two local analyses together with the boundary conditions to obtain a global description of the solution. The principle obstacle in completing this jigsaw puzzle is that while the "outer," WKB solution is always a sum of $W_+(x)$ and $W_-(x)$, the coefficients of the sum are *different* in different portions of the complex plane—Stokes' phenomenon. Thus, in order to make the final answer intelligible, it is necessary to digress briefly and explain this.

C. Stokes' phenomenon

If the WKB solutions $W_+(x)$ and $W_-(x)$ are written in the symbolic form

$$W(x) = Q^{-1/4}(x)e^{P(x)}, \quad (6.7)$$

then the Stokes lines are defined by,[16]

$$\mathrm{Im}[P(x)] = \text{const}, \quad (6.8)$$

and the anti-Stokes lines by

$$\mathrm{Re}[P(x)] = \text{const}. \quad (6.9)$$

On the Stokes lines, which will be indicated on the graphs below by *solid* lines, the WKB solutions grow or decay *exponentially* without change of phase. The anti-Stokes lines are curves of purely sinusoidal behavior: $W(x)$ oscillates without change of amplitude. To emphasize the oscillatory character of the WKB solutions upon them, the *anti-Stokes* curves will be graphed as *wavy* lines.

The heart of Stokes' phenomenon is that while $u(x)$ can always be represented as

$$u(x) \sim aW_-(x) + bW_+(x) \quad (6.10)$$

(except near a transition point), the coefficients must be different in different sectors of the complex plane. Within the sector bounded by adjoining anti-Stokes lines A_1 and A_2, one WKB solution (let it be $W_-(x)$ for definiteness) will be exponentially large ("dominant") in comparison to the other, which is said to be "subdominant" in that sector. It then follows that b in (6.10), because of the smallness of $W_+(x)$, can be arbitrary without violating the formal asymptotic equality because exponentially small quantities are com-

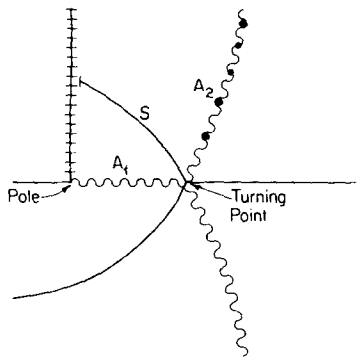

FIG. 4. The Stokes lines (solid) and anti-Stokes lines (wavy) for $\lambda = 1/100$. The branch line is marked with crosscuts. Black dots mark the zeros of the Whittaker function.

pletely ignored in Poincaré's definition of asymptotic relations. On the anti-Stokes lines, however, b must assume definite (and usually different) values because W_+ is the same magnitude as W_- upon them. Stokes established the convention[17] that the coefficient of the subdominant solution jumps from $b\,(A_1)$ to $b\,(A_2)$ as one crosses the Stokes line between them. This convention ensures that (6.10) will be numerically accurate near, as well as on, A_1 and A_2, and also, since W_+ is smallest in comparison to W_- on the Stokes line, that when b jumps, the corresponding jump in $u(x)$ is as small as possible.

The Stokes and anti-Stokes lines for the solutions of (1.1) for λ positive and real are shown in Fig. 4. Three Stokes and three anti-Stokes lines radiate from the turning point, but one of each ends on the branch line, so only two Stokes and two anti-Stokes lines radiate to infinity. Their number (two of each) is consistent with what one would have deduced directly from

$$u_{xx} - \lambda u = 0, \tag{6.11}$$

which approximates (1.1) as $|x| \to \infty$; parenthetically, we note that only these surviving pairs are relevant when performing the joint or "Whittaker" matching described above.

Making the simplifying assumption $A = -\infty$, justified previously, let us look first at the Stokes line radiating from the pole leftward to $x = -\infty$. Since $W_+(x)$ blows up exponentially along this Stokes line, b in (6.10) must be zero and $u(x)$ proportional to W_- alone, so that the boundary condition at $x = -\infty$ can be satisfied.

Since the coefficient of $W_+(x)$ can only jump to a nonzero value on a Stokes line, it follows that

$$u(x) \sim W_-(x) \quad \text{on } A_1, \tag{6.12}$$

which is the anti-Stokes line connecting the two points. The argument of the exponential in (6.1) is now pure imaginary, implying sinusoidal behavior. Dickinson[3] shows that, physically, (6.12) correponds to a Rossby wave propagating towards the pole and being *absorbed* there. So far so good, but (6.12) brings us face to face with an apparent paradox: how can a single complex exponential ever satisfy the boundary condition?

The answer is that it cannot; Stokes' phenomenon saves the day by forcing b to jump to a new nonzero value on the Stokes line S in Fig. 4. The new value of b is determined in two steps. First, the proper Airy function approximation to $u(x)$ in the vicinity of the turning point is found by demanding that it asympototically match to (6.12) along the anti-Stokes line A_1. Then, $b\,(A_2)$ is determined by matching the "inner" Airy approximation to the "outer" WKB solution along the anti-Stokes line A_2.

The matching is routine, but the result is not. The Airy functions $\mathrm{Ai}(x)$ and $\mathrm{Bi}(x)$ are both standing waves for x negative and real. This is fine for the quantum harmonic oscillator problem in which the other transition point is also a turning point; the two turning points reflect the wave back and forth between them to create the standing wave. Here, however, as shown by Dickinson,[3] the transition point at $x = 0$ is a perfect *absorber*.

The function that correctly matches to (6.12) is $\mathrm{Ai}(ze^{2\pi i/3})$ where $z \equiv \lambda^{2/3}(x - x_t)$, which has the asymptotic approximations

$$\mathrm{Ai}(ze^{2\pi i/3}) \sim \frac{e^{i\pi/12}}{2\pi^{1/2}|z|^{1/4}} e^{i\frac{2}{3}|z|^{3/2}}, \quad \arg z = \pi[\text{on } A_1],$$
$$\sim \frac{1}{\pi^{1/2}|z|^{1/4}} \cos\left[\tfrac{2}{3}|z|^{3/2} - \pi/4\right],$$
$$\arg z = \frac{\pi}{3}[\text{on } A_2]. \tag{6.13}$$

The reader can easily verify that these large $|x|$ limits of the "inner" solution are identical with the $|x - x_t| \to 0$ limits of the WKB approximations along A_1 and A_2, where the former is given by (6.12) and the latter is found by matching with (6.13) to be

$$u(x) \sim Q(x)^{-1/4} e^{-i\pi\kappa} \cos[2\kappa\phi\,(\lambda x) - \kappa\pi - \pi/4]. \tag{6.14}$$

This plainly has an infinite number of zeros along the anti-Stokes line A_2 which are schematically denoted by the black dots in Fig. 4.

Unfortunately, when λ is real (as assumed for clarity above), all theses zeros are in the upper half-plane and are perfectly useless for satisfying the boundary condition at $x = B$ on the real axis. One can see now why the eigenvalue must be complex: when λ is moved into the upper half-plane (as consistent with Theorem 3 above), the turning point x_t is moved into the lower half-plane. It is then possible to make one of the zeros along A_2 coincide with the real axis.

Figure 5 shows the Stokes and anti-Stokes lines of the fourth mode for $B = 100$. The Whittaker function has three roots below the real axis, an infinite number above, and its fourth root along A_2 is real and satisfies the boundary condition at $x = B$.

We will see in the next section that "double Bessel" matching gives extremely accurate approximations to the low-order eigenvalues and eigenfunctions, but (6.14) must fail as $n \to \infty$ for fixed B, because as we have already seen $|\lambda| \to \infty$ in this limit. In turn, this implies that $|x_t| \to 0$, and when the turning point and the pole become too close together, it is no longer sensible—either physically or mathematically—to separate near-the-pole behavior from near-the-turning point behavior. The "Whittaker" matching is free from this defect and can in fact reproduce all the results of

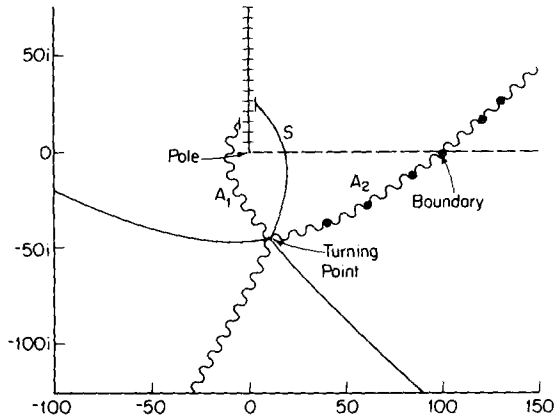

FIG. 5. The Stokes lines (solid) and anti-Stokes lines (wavy) for the fourth mode for $B = 100\,(\lambda = 0.0050 + 0.0208i)$. As in Fig. 4, the branch line is marked with crosscuts, and the zeros of the Whittaker function with black dots. The fourth root is on the real axis at $x = B$ so that the boundary condition is satisfied.

Sec. 4 on high-order modes if one relaxes the assumption $A = -\infty$. In practice, however, as shall be seen in the next section, the "double Bessel" matching gives acceptable accuracy when $|\lambda| < 1$, which turns out to include the range of n and B which is of primary physical interest.

D. Simplification of the "double Bessel" eigenrelation

The vanishing of (6.13) at $x = B$ is equivalent to the eigenrelation

$$2\kappa\phi\,(\lambda B) - \kappa\pi = (n - \tfrac{1}{4})\,\pi, \tag{6.15}$$

where n is a positive integer, the mode number. One can eliminate the $\sin^{-1}$ implicit in $\phi(y)$ by letting

$$\lambda = \sin^2\tau/B, \tag{6.16}$$

which transforms (6.14) to

$$\tau + \sin\tau\cos\tau - \tfrac{1}{2}\pi = \left[(n - \tfrac{1}{4})/B^{1/2}\right]\pi\sin\tau. \tag{6.17}$$

What is striking about (6.16) is τ is not a function of B or n alone, but is rather a function of the single parameter

$$q \equiv (n - \tfrac{1}{4})/B^{1/2}. \tag{6.18}$$

This implies that, just as with (5.7), the solutions of (6.17) are identical for all modes with appropriate rescaling of axes, i. e.,

$$\lambda_n(B) = \frac{9}{(4n-1)^2}\,\lambda_1\left[\frac{9B}{(4n-1)^2}\right]. \tag{6.19}$$

E. The "Airy" approximation

Equation (6.17) has the drawback that it is only an *implicit* equation for λ. When the parameter

$$\sigma \equiv e^{\pi i/3} d_n/B^{1/3} \tag{6.20}$$

is small, however, where

$$d_n \equiv \left|\tfrac{3}{8}\pi(4n-1)\right|^{2/3}, \tag{6.21}$$

one can solve (6.17) by a power series in σ to obtain

$$\lambda = (1/B)(1 + \sigma + \cdots), \tag{6.22}$$

or in exponential form

$$\lambda = e^{\sigma}/B. \tag{6.23}$$

Equation (6.23) is the "Airy approximation" given in (5.7) and the abstract; empirically (not systematically) it was found that the exponential form was much more accurate than the power series (6.22) for moderate σ, but both are *exact* in the limit $B \to \infty$ for fixed n, i. e., the limit $\sigma \to 0$.

The reason for the name "Airy approximation" is that in the limit $B \to \infty$ (5.7) shows that $\lambda \to 0$, implying that $|x_t| \to \infty$. Thus, the turning point and the pole move away from each other in this limit, and the radius over which the inner approximation, i. e.,

$$u(x) \sim \mathrm{Ai}(ze^{2\pi i/3}), \tag{6.24}$$

where

$$z = \lambda^{2/3}(x - x_t), \tag{6.25}$$

is valid, becomes larger and larger (in terms of $|z|$). Thus, the first few zeros of (6.13) are really the first few zeros of the Airy function (6.24). These are known constants, however, and the d_n given by (6.21) are in fact the nth roots of $\mathrm{Ai}(-z)$.[18] The approximation (6.22) is precisely what one would obtain by determining λ so as to make $x = B$ coincide with the nth root of the Airy function (6.24)—hence the name "Airy approximation" for (6.22) and (6.23), the latter being the form we shall actually use.

7. ACCURACY OF WKB

Much of the books on asymptotic approximations by Dingle and Olver is almost morbidly concerned with formal error terms and bounds, but this elaborate machinery is not useful here. The error in our approximate eigenmodes is not merely due to truncating an asymptotic series at lowest order but also depends on the accuracy of the value of λ which is used to evaluate the WKB expression. In turn, the error in λ may be large or small in comparison to the accuracy of the WKB approximation at the boundaries. Thus, the simplest and most reliable way to see how well WKB works is to compare the approximate results with the exact answers obtained by brute force numerical solution of (1.1).

The three eigenvalue approximations compared are

$$\tau + \sin\tau\cos\tau - \tfrac{1}{2}\pi = \left[\frac{(n-\tfrac{1}{4})}{B^{1/2}}\right]\pi\sin\tau - i\ln\left[\Omega\left(\frac{B^{1/2}}{2\sin\tau}\right)\right] \quad \begin{bmatrix}\text{Whittaker}\\ \text{matching}\end{bmatrix}, \tag{7.1}$$

where

$$\Omega(\kappa) = (2\pi)^{1/2}\kappa^{1/2+\kappa}e^{-\kappa}/\Gamma(1+\kappa); \tag{7.2}$$

$$\lambda = \frac{\sin^2\tau}{B}\tau, \tag{7.3}$$

$$\tau + \sin\tau\cos\tau - \tfrac{1}{2}\pi = \left[\frac{(n-\tfrac{1}{4})}{B^{1/2}}\right]\pi\sin\tau \quad \begin{bmatrix}\text{double}\\ \text{Bessel}\\ \text{matching}\end{bmatrix} \tag{7.4}$$

with λ again related to τ through (7.3); and

$$\lambda = (1/B)e^{\sigma} \quad \text{(Airy approximation)}, \tag{7.5}$$

$$\sigma = \frac{e^{\pi i/3}}{B^{1/3}}\left|\tfrac{3}{8}\pi(4n-1)\right|^{2/3}. \tag{7.6}$$

TABLE I. A comparison of the exact and approximate eigenvalues λ for the lowest mode with $A = -\infty$ and various B. "Whittaker" refers to the WKB approximation with coefficients determined by matching with the asymptotics of the Whittaker function; "Double Bessel" is the WKB determined through matching the two local Bessel function approximations.

	Re(λ)	Im(λ)	$\lvert\lambda\rvert$	Phase	Relative Errors $\lvert\lambda\rvert$	Phase
$B = 100$	$\lvert\sigma\rvert = 0.50$					
Exact	0.011 58	0.005 50	0.012 81	25.407		
Whittaker	0.011 56	0.005 46	0.012 78	25.270	0.26%	0.54%
Double Bessel	0.011 61	0.005 47	0.012 83	25.231	0.14%	0.69%
Airy	0.011 66	0.005 39	0.012 84	24.804	0.19%	2.4 %
$B = 40$	$\lvert\sigma\rvert = 0.68$					
Exact	0.028 75	0.019 89	0.034 96	34.674		
Whittaker	0.028 69	0.019 73	0.034 82	34.525	0.40%	0.43%
Double Bessel	0.028 92	0.019 83	0.035 07	34.444	0.31%	0.66%
Airy	0.029 21	0.019 45	0.035 10	33.664	0.40%	2.9 %
$B = 10$	$\lvert\sigma\rvert = 1.08$					
Exact	0.095 96	0.1400	0.1696	55.660		
Whittaker	0.095 21	0.1389	0.1684	55.571	0.68%	0.16%
Double Bessel	0.097 62	0.1420	0.1723	55.494	1.6 %	0.29%
Airy	0.1021	0.1376	0.1713	53.439	1.1 %	4.0 %
$B = 4$	$\lvert\sigma\rvert = 1.46$					
Exact	0.1218	0.4960	0.5107	76.203		
Whittaker	0.1200	0.4919	0.5063	76.288	0.86%	0.11%
Double Bessel	0.1252	0.5200	0.5349	76.465	4.7 %	0.34%
Airy	0.1559	0.4952	0.5192	72.527	1.7 %	4.8 %
$B = 1$	$\lvert\sigma\rvert = 2.32$					
Exact	− 1.691	2.675	3.164	122.311		
Whittaker	− 1.712	2.644	3.150	122.927	0.46%	1.1%
Double Bessel	− 2.269	3.311	4.014	124.426	27. %	3.7%
Airy	− 1.355	2.888	3.190	115.130	0.82%	12. %
$B = 0.4$	$\lvert\sigma\rvert = 3.15$					
Exact	− 12.46	3.241	12.88	165.420		
Whittaker	− 12.59	3.146	12.98	165.966	0.77%	0.33%
Double Bessel	− 22.73	8.838	24.39	158.753	89. %	45. %
Airy	− 11.05	4.861	12.07	156.255	6.2 %	63. %

The first two approximations are *implicit* and (7.1) and (7.4) must be solved analytically or by perturbation theory; the Airy approximation is *explicit*. The Whittaker matching eigenrelation differs from that from double Bessel matching by only a single term, but that term causes the solution of (7.1) to depend on n and B *independently* instead of through a *single* parameter formed of B and n. Thus, (5.10) is true of the second and third approximations above (7.4) and (7.6) but not the first (7.1).

Physically, one is primarily interested in $n \leqslant 3$ and $B \geqslant 4$ since smaller values of B would correspond to unrealistically large (supersonic) winds, and $n > 3$ is rarely observed in the stratosphere. Dickinson[3] thoroughly discusses the physics of the atmospheric wave problem that motivated this work. Some controversies have arisen and it has been argued that Dickinson's WKB reasoning is rubbish because WKB is not sufficiently accurate to handle such singular SL problems of the fourth kind. It is thus a matter of physics—not merely numerical analysis—to examine the accuracy of our approximations.

Tables I through III compare the exact and approximate eigenvalues for the lowest three modes. The Whittaker-matched eigenrelation is the numerical star; the relative error is no worse than 1.1% for any of the values tabulated. The price is greater complexity (a Γ function of complex argument) and loss of insight because the near-turning-point and near-the-pole behaviors are lumped together into a single inner solution, and also because of the loss of (5.10) which shows that the curves $\lambda_n(B)$ all have similar shape for small n.

The double Bessel-matched approximation, though poorer, is still quite acceptable. In the range of physical interest, $n \leqslant 3$ and $B \geqslant 4$, the error is no worse than 10% in absolute value and 5% in phase. Both this and the Airy approximation—but not (7.1)—lose accuracy as σ (and therefore $|\lambda|$) increase where σ is defined by (6.20). For fixed B, σ increases as n increases as noted in the tables; so the tables for $n = 2$ and $n = 3$ are shorter than that for $n = 1$ to remind us that (7.4) and (7.5) are useful for an ever narrower range of B as the mode number becomes larger.

The Airy approximation (7.5) is the crudest of all, but it is still amazing that an explicit approximation of this simplicity can work so well for a problem whose differential equation is singular. For $n = 1$, the errors are less than 12% even for $B = 1$, so (7.5) is a good description of the entire hodograph in Fig. 3.

The approximate and exact eigenfunctions for the lowest mode are compared in Figs. 6, 7, and 8. Again, accuracy improves as B increases just as for λ, but the agreement is still remarkable.

Why does WKB work so well? The method of multiple scales,[14,15] which is one of many alternative ways of justify-

TABLE II. A comparison of the exact and approximate eigenvalues λ for the second mode with $A = -\infty$ and various B.

	Re(λ)	Im(λ)	$\lvert\lambda\rvert$	Phase	Relative $\lvert\lambda\rvert$	Errors Phase
$B = 100$	$\lvert\sigma\rvert = 0.88$					
Exact	0.010 97	0.010 99	0.015 52	45.047		
Whittaker	0.010 95	0.010 95	0.015 49	45.001	0.24%	0.10%
Double Bessel	0.010 99	0.010 98	0.015 33	44.972	0.04%	0.17%
Airy	0.011 23	0.010 71	0.015 52	43.635	0.00%	3.1 %
$B = 40$	$\lvert\sigma\rvert = 1.19$					
Exact	0.021 59	0.040 24	0.045 66	61.785		
Whittaker	0.021 56	0.040 18	0.045 60	61.789	0.14%	0.34%
Double Bessel	0.021 70	0.040 42	0.045 88	61.769	0.47%	0.02%
Airy	0.023 23	0.039 01	0.045 41	59.222	0.56%	4.1 %
$B = 10$	$\lvert\sigma\rvert = 1.89$					
Exact	− 0.050 09	0.2729	0.2775	100.400		
Whittaker	− 0.050 33	0.2725	0.2771	100.466	0.15%	0.08%
Double Bessel	− 0.052 92	0.2789	0.2839	100.743	2.3 %	0.43%
Airy	− 0.018 03	0.2572	0.2579	94.010	7.1 %	8.0 %
$B = 4$	$\lvert\sigma\rvert = 2.57$					
Exact	− 0.8611	0.8200	1.189	136.398		
Whittaker	− 0.8625	0.8183	1.189	136.507	0.01%	0.25%
Double Bessel	− 0.9428	0.8704	1.283	137.286	7.9 %	2.0 %
Airy	− 0.5516	0.7165	0.9043	127.590	24. %	20. %
$B = 1$	$\lvert\sigma\rvert = 4.08$					
Exact	− 19.37	0.1890	19.37	179.441		
Whittaker	− 19.38	0.1870	19.38	179.447	0.05%	1.1 %
Double Bessel	− 24.44	3.376	24.68	172.136	27. %	1300. %
Airy	− 7.11	− 2.950	7.698	− 157.463	60. %	Hopeless

ing WKB (away from transition points), provides an amusing and ironic answer.

In brief, the multiple scale argument states that the faster the eigenfunction oscillates, i. e., the greater the ratio of the "slow" scale on which the coefficients of the differential equation vary to the "fast" scale on which $u(x)$ itself is oscillating, the better the accuracy of the WKB approximation. The WKB eigencondition for a normal SL problem is that the total phase change on $[A,B]$ is $n\pi$, so the eigenfunction obviously oscillates more rapidly as n increases. In practice, this means that WKB is poor for the lowest mode, fair for moderate n, and superb for large n.

For the lowest mode of a singular SL problem of the fourth kind, however, the total phase change is usually greater than π and increases steadily with B. Figures 6 through 9 show that the real part of the lowest mode has no interior zeros for $B = 1$, one for $B = 5$, two for $B = 20$, and no fewer than four for $B = 100$. (The imaginary part oscillates similarly, but its roots coincide with those of the real part only at $x = B$). Because the eigenfunction graphed in Fig. 9 oscil-

TABLE III. A comparison of the exact and approximate eigenvalues λ for the third mode with $A = -\infty$ and various B.

	Re(λ)	Im(λ)	$\lvert\lambda\rvert$	Phase	Relative $\lvert\lambda\rvert$	Errors Phase
$B = 100$	$\lvert\sigma\rvert = 1.19$					
Exact	0.008 63	0.016 00	0.018 18	61.661		
Whittaker	0.008 70	0.016 04	0.018 25	61.525	0.41%	0.22%
Double Bessel	0.008 73	0.016 08	0.018 29	61.500	0.64%	0.26%
Airy	0.009 34	0.015 53	0.018 12	58.980	0.33%	4.3 %
$B = 40$	$\lvert\sigma\rvert = 1.61$					
Exact	0.005 20	0.058 13	0.058 36	84.886		
Whittaker	0.005 22	0.058 11	0.058 35	84.867	0.03%	0.02%
Double Bessel	0.005 22	0.058 48	0.058 71	84.904	0.60%	0.02%
Airy	0.009 68	0.055 16	0.056 01	80.048	4.0 %	5.7 %
$B = 10$	$\lvert\sigma\rvert = 2.56$					
Exact	− 0.3559	0.3401	0.4923	136.300		
Whittaker	− 0.3562	0.3398	0.4923	136.344	0.01%	0.03%
Double Bessel	− 0.3698	0.3477	0.5076	136.766	3.1 %	1.1 %
Airy	− 0.2169	0.2871	0.3598	127.068	27. %	21. %
$B = 4$	$\lvert\sigma\rvert = 3.48$					
Exact	− 3.086	0.7583	3.178	166.194		
Whittaker	− 3.087	0.7579	3.179	166.206	0.03%	0.01%
Double Bessel	− 3.365	0.8694	3.475	165.513	9.4 %	4.9 %
Airy	− 1.409	0.1866	1.421	172.457	55. %	45. %

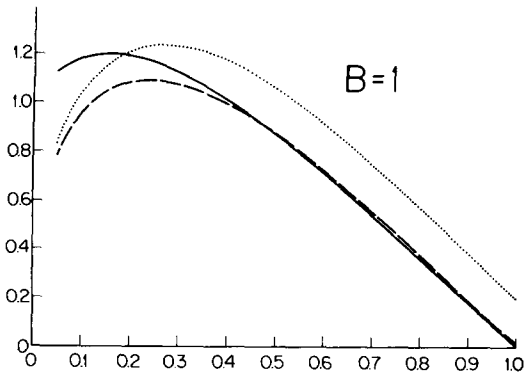

FIG. 6. A comparison of the exact (solid line), jointly (Whittaker) matched WKB (dashed line), and separately matched (double Bessel) WKB (dotted line) graphs for the real part of the lowest mode for $A = -\infty$, $B = 1$.

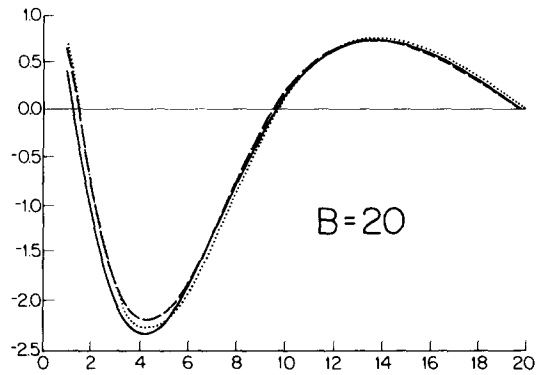

FIG. 8. A comparison of the exact (solid line), Whittaker-matched WKB (dashed line), and double Bessel-matched WKB (dotted line) graphs for the real part of the lowest mode for $A = -\infty$, $B = 20$.

lates as rapidly as the fifth mode (four interior zeros) of a normal SL problem, the WKB approximation to it has the same accuracy as for the fifth mode of a nonsingular equation—but it is the lowest mode nonetheless.

This increasing phase variation with B can be seen by noting that as $B \to \infty$ and $\lambda \to 0$ proportional to $1/B$ (from 7.5), one can approximate (1.1) over an increasingly large interval by

$$u_{xx} + (1/x)u = 0, \tag{7.7}$$

whose asymptotic approximation [matching to (6.12)] is proportional to

$$x^{1/4} e^{-2ix^{1/2}}. \tag{7.8}$$

The scale of the oscillation thus varies with x, but the total phase change on $[0,B]$ is obviously $O(2B^{1/2})$. [Using (6.1), one can show more precisely that the total phase change is $(\pi/2)B^{1/2}$ plus terms vanishing as $B \to \infty$.] Thus, WKB must inevitably improve for a given mode as B increases.

The Whittaker matched WKB, seen from the tables to be very good for small n, does but improve for large n; as noted earlier, it can—if we relax the restriction $A = -\infty$ inherent in (7.1)—reproduce all the results of Sec. 4 for higher-order modes as well. The double Bessel and Airy approximations fail for large n, but this is not the fault of the WKB per se. Rather, we have obtained (7.4) from (7.1) by replacing the complex gamma function by its approximation for large argument, and (7.5) from (7.4) by applying Taylor expansions in σ—both non-WKB simplifications.

Thus, the Whittaker-matched WKB works for all n here whereas WKB is successful only for large n for a Type I problem. Thus, we are led to an amusing and ironic conclusion: WKB actually works *better* for *singular* eigenproblems of Type IV than for the conventional nonsingular Sturm–Liouville equations of the classes so thoroughly studied in the past.

8. THE COMPLETE SPECTRUM

So far, we have looked at the small n and large n modes separately, the former with the additional assumption that $A = -\infty$. It is now appropriate to tie these ideas together by looking at a dozen chosen modes for a typical case ($A = -6$, $B = 6$). The eigenvalues are listed in Table 4, and Fig. 10 shows the lowest nine values of $\lambda^{1/2}$, which is graphed instead of λ itself for visual clarity. The modes can be grouped into three categories.

First, the four modes marked by *'s in the second column of the table (and by triangles in Fig. 10) are shining examples of the low-order modes discussed in Sec. 5. The ratio of the coefficient of $W_{-\kappa,\frac{1}{2}}$ to that of $M_{-\kappa,\frac{1}{2}}$, tabulated in the third column, is very large. The exact eigenvalues for

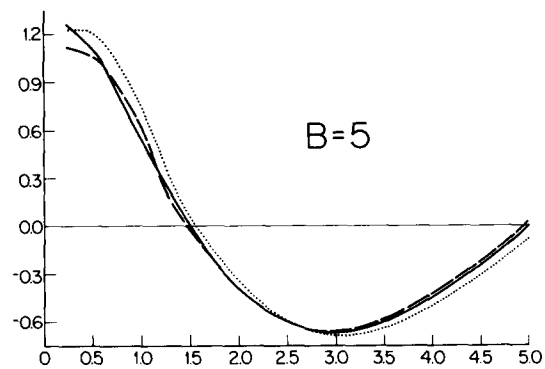

FIG. 7. A comparison of the exact (solid line), Whittaker-matched WKB (dashed line), and double Bessel-matched WKB (dotted line) graphs for the real part of the lowest mode for $A = -\infty$, $B = 5$.

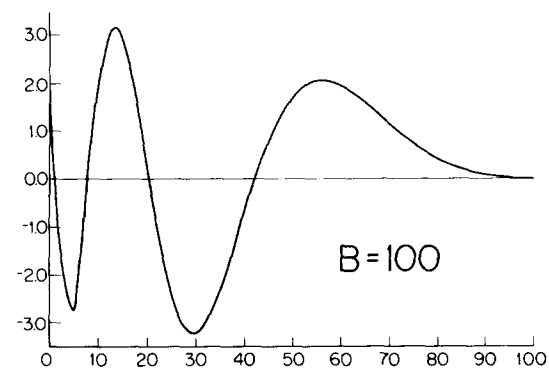

FIG. 9. The real part of the lowest mode for $B = 100$.

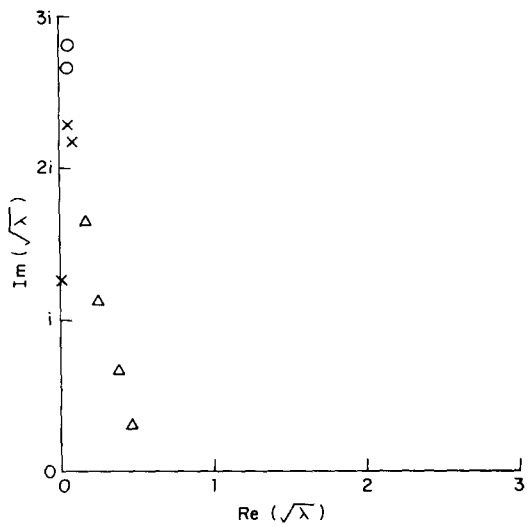

FIG. 10. The square root of λ (*not* λ itself) is shown for the lowest nine modes on $[-6,6]$. The four modes marked with triangles are well approximated by the corresponding eigenvalues for $[-\infty, 6]$. The two eigenvalues marked by circles are well approximated by (4.5). The crosses represent intermediate modes for which no simple approximation is known.

$A = -6$ are well approximated (to within 4%) by those for $A = -\infty$, which are given on the second line of each entry for these four asterisked modes.

The last five modes in the table (circles in Fig. 10) are examples of the large n dikeric modes discussed in Sec. 4. The second line of each entry for these five gives the approximate eigenvalues computed via (4.5) with that value of m which is given in the second column. Note that in this case $m = n + 2$, where n is the mode number determined by ordering the modes according to $|\lambda|$. For a normal SL problem, of course, $m = n$. Since (4.6) gives a purely real answer, the relative error in $\mathrm{Im}(\lambda)$ is infinite, but the absolute errors in both the real and imaginary parts are small in comparison to $|\lambda_n - \lambda_{n+1}|$ and decrease *algebraically* [as does $\mathrm{Im}(\lambda)$ itself as $n \to \infty$].

The three modes marked "Intermediate" in the table (crosses in Fig. 10) are hybrids of the two classes above. Whittaker-matched WKB would give an eigenrelation for them, but it would be both implicit and messy. As noted in the table, no simple explicit approximation is available for these modes.

Mode 4 is interesting because (i) it interrupts the pattern of the low-order monokeric modes which are well approximated by their counterparts for $A = -\infty$ and (ii) $\mathrm{Im}(\lambda_4)$ is almost zero. As noted in Sec. 2, Theorem 3 shows that $\mathrm{Im}(\lambda) = 0$ is possible only when $u(x)$ in effect satisfies three boundary conditions which can occur only on a set of measure zero in (A, B, n) parameter space. Here, the fourth mode—through sheer luck—happens to be close to one of these cases.

Modes 6 and 7 are interesting because, although they are nearly degenerate (i. e., $\lambda_6 \approx \lambda_7$) here—in contrast to the widely spaced eigenvalues of a normal one-dimensional SL eigenproblem with nonperiodic boundary conditions—they diverge wildly as the parameters are changed. For example, when $|A|$ is increased (with B fixed), the seventh mode—the one with the *higher* n and smaller ratio of W/M initially—rapidly becomes a pure monokeric mode like that illustrated in Fig. 12 (top). [At $A = 7$, $W/M = 13.4$ and $\lambda_7 = (-4.855, .5060)$, which differs little from its asymptotic ($A = -\infty$) value of $(-4.931, .4375)$.] The sixth mode, which is closer to a monokeric mode initially, behaves in a completely opposite fashion: the ratio W/M *decreases* very rapidly until it falls to *zero* at $A = -7.008$ where $\lambda_6 = (-3.743, 0)$. Thus, ($n = 6$, $A = -7.008$, $B = 6$) is one of the members of that set of measure zero, where λ is real and the eigenfunction, being proportional to $M_{-\kappa,\frac{1}{2}}$ alone, is an entire function.

Thus, these intermediate modes show that there is not a monotonic transition from the limiting behavior for small n to the limiting behavior for large n; rather, there can be some interleaving of the two. It is for this reason that the terms "monokeric" and "dikeric" were introduced earlier. Although the $n = 1$ mode is monokeric, i. e., exponentially decaying for $x < 0$ (unless A and B are both too small to be relevant to the original physical problem), and although one can prove that as $n \to \infty$ the modes must be dikeric, i. e., oscillatory on both sides of $x = 0$, modes of *moderate* n may resemble *either* graph in Fig. 2 or some hybrid of the two.

9. SUMMARY: A COMPARISON OF NORMAL AND SINGULAR STURM–LIOUVILLE EIGENPROBLEMS

The principal provable similarities between the first and fourth classes of Sturm–Liouville problems are the following. First, the eigenfunctions are orthogonal. Second, in the limit $n \to \infty$, the eigenfunctions and eigenvalues are essentially the same with or without the $1/x$ term in the differential equation. For finite n, there is (i) a small boundary layer about $x = 0$ and (ii) a nonzero imaginary part of the eigenvalue if the pole is present, but these disappear in the limit.

The principal differences are the following. First, the eigenvalues and eigenfunctions of a nonsingular, self-adjoint Sturm–Liouville eigenproblem are always real. Here, however, in spite of the fact that the problem is still self-adjoint, the eigenvalues and eigenfunctions are both *complex*.

Second, the modes of a Sturm–Liouville eigenproblem of the first kind can be characterized by their nodes: the nth mode has exactly $(n - 1)$ zeros on the interior of $[A,B]$.[2] Here, however, the real and imaginary parts of the low-order eigenfunctions have an ever increasing number of zeros as $B \to \infty$ with n fixed. The real part of the lowest mode for $B = 100$, illustrated in Fig. 9, has no fewer than four interior zeros, for example. Nor do the higher modes escape. The integer m which appears in the asymptotic ($n \to \infty$) eigenvalue formula (4.5) is generally different from the mode number n, where the latter is determined by ordering the eigenvalues according to $|\lambda|$. Thus, the $n = 8$ mode of Table IV has nine interior zeros instead of the expected seven. As explained in Sec. 7, this tendency of the singular modes of a given n to oscillate more rapidly than their counterparts for a nonsingular equation makes the WKB method actually work better, sometimes much better, for Sturm–Liouville problems of the fourth kind than for the nonsingular and seemingly more amenable equations of the first kind.

TABLE IV. The eigenvalues for $A = -6, B = 6$. The mode number n, the integer m which appears in (7.7) (if applicable), the absolute value of the ratio of the coefficient of $W_{-\kappa,\frac{1}{2}}$ to that of $M_{-\kappa,\frac{1}{2}}$, the approximate eigenvalues obtained by either setting $A = -\infty$ (for the purely singular modes) or using (4.5) for large n modes, and the relative errors of the approximations are also shown. Monokeric modes are indicated by asterisk in the second column.

					Relative Errors	
n	m	W/M	Re(λ)	Im(λ)	Re(λ)	Im(λ)
1	*	1.06E5	0.1251	0.2850		
		($A = -\infty$)	0.1251	0.2850	0.0%	0.0%
2	*	2.34E4	−0.2967	0.5203		
		($A = -\infty$)	−0.2971	0.5204	0.2%	0.02%
3	*	141.4	−1.218	0.5634		
		($A = -\infty$)	−1.225	0.5626	0.7%	0.12%
4	—	0.402	−1.602	0.0078		
			(Intermediate—No Simple Approximation)			
5	*	18.6	−2.726	0.4900		
		($A = -\infty$)	−2.781	0.5101	2.0%	4.1%
6	—	4.61	−4.717	0.3324		
			(Intermediate—No Simple Approximation)			
7	—	2.48	−5.224	0.2186		
			(Intermediate—No Simple Approximation)			
8	10	2.40	−7.156	0.2323		
			Eq. (4.5) −6.85	0.0000	4.3%	∞
9	11	3.20	−7.996	0.3123		
			Eq. (4.5) −8.29	0.0000	3.7%	∞
10	12	1.74	−10.14	0.1813		
			Eq. (4.5) −9.87	0.0000	2.7%	∞
38	40	0.517	−109.791	0.0333		
			Eq. (4.5) −109.662	0.0000	0.11%	∞
98	100	0.241	−685.454	0.0076		
			Eq. (4.5) −685.389	0.0000	0.01%	∞

Third, the eigenvalues—all eigenvalues—of a normal one-dimensional Sturm–Liouville equation with nonperiodic boundary conditions are well separated. Here, however, $\lim_{B\to\infty}\lambda_n = 1/B$ for all fixed n (see Sec. 5) so that the eigenvalues of the lowest few modes cluster about a common value and become quasidegenerate. Furthermore, the proportionality to $1/B$ is different from the $1/B^2$ [strictly, $1/(B-A)^2$] for a given λ_n of a first kind eigenproblem in this same limit.

These differences and similarities are provocative, but a number of important questions remain for future research. First, completeness. It is plausible, especially in view of their asymptotic identity with ordinary sine functions, to suppose that the modes are complete at least for the original partial differential equation which gave rise to this problem. The possibility of expanding an *arbitrary* analytic function, however, in terms of a series of *singular* functions like the modes of (1.1) raises fascinating questions that I will not attempt to answer here.

Second, one may ask: would the conclusions given above all hold if the first-order pole in (1.1) were replaced by a second-order pole or some other species of singularity? (Olver[19] has made a start on this). Clearly, a rich harvest awaits the future in these Sturm–Liouville eigenproblems of the fourth kind.

ACKNOWLEDGMENTS

I would like to thank Robert E. Dickinson and K. K. Tung for inspiring this problem. Both of them and Richard S. Lindzen provided helpful discussions. I also wish to thank the referee for his comments which have greatly improved the readability of this paper and made it accessible to a wider audience. This work was supported by N. S. F. grant OCE-79-09191 and NASA grant NSG-7209 at The University of Michigan and by NASA grant NGL-22-007-228 at Harvard. I am appreciative of the hospitality extended to me by Professor Richard Lindzen at Harvard where this work was completed.

APPENDIX A: CONFLUENT HYPERGEOMETRIC FUNCTIONS

The Whittaker functions of Sec. 2 are related to the standard confluent hypergeometric functions by the identities

$$M_{-\kappa,\frac{1}{2}}(y) = e^{-y/2} y M(1+\kappa,2,y), \tag{A1}$$

$$W_{-\kappa,\frac{1}{2}}(y) = e^{-y/2} y U(1+\kappa,2,y), \tag{A2}$$

which have the power series representations

$$M(1+\kappa,2,y) = \sum_{m=0}^{\infty} \frac{(1+\kappa)_m}{(2)_m}\frac{y^m}{m!} = 1 + \frac{1+\kappa}{2}y + \frac{(1+\kappa)(2+\kappa)}{12}y^2 + \cdots, \tag{A3}$$

$$U(1+\kappa,2,y) = \frac{1}{\Gamma(1+\kappa)}\left(\frac{1}{y} + \kappa M(1+\kappa,2,y)\log y + \kappa\sum_{m=0}^{\infty}\frac{(1+\kappa)_m}{(2)_m}\frac{y^m}{m!}\left[\psi(1+\kappa+m) - \psi(1+m) - \psi(2+m)\right]\right), \tag{A4}$$

where

$$(x)_m = x(x+1)\cdots(x+m-1), \tag{A5}$$

and $\psi(x)$ is the logarithmic derivative of the gamma function ("digamma" function). The reason for the factor of $\Gamma(1+\kappa)$ in (3.6) is to eliminate the corresponding factor in (A4).

The corresponding asymptotic approximations for fixed κ, $y \to \infty$, are given by (4.1) and (4.2) above.

As a final note, the formulas of the paper require computing two transcendental functions—$\sin^{-1}(z)$ and $\Gamma(z)$—for *complex* argument. For the former, however, identity 4.4.37 of Abramowitz and Stegun[20] reduces the task to evaluating (i) the complex logarithm, which is a built-in library function on most computers and (ii) the arcsine function for a *real* argument between 0 and 1, which can be done via the polynomial approximation 4.4.46 of Abramowitz and Stegun.[20] The complex gamma function can be evaluated by using its well-known recursion relation $\Gamma(z+1) = z\Gamma(z)$ to march out to large z, using its known asymptotic expansion, and then marching back the same way. A FORTRAN program to do this is given by Lucas and Terril.[21]

APPENDIX B: THE DISCRETE AND CONTINUOUS SPECTRUM

There are two fundamentally different ways of analyzing the inviscid limit. The first, adopted by Dickinson[3] is the continuum modes approach. This has the great advantage that all the arithmetic is real, but it has the disadvantage that any physically realizable solution is an *integral* over the *real* eigenvalue λ. For the special case of a δ-function lower boundary forcing, he was able to perform the integrals via stationary phase.

Unfortunately, the need for λ integration implies that a continuum mode—i. e., a Whittaker function for some particular real value of λ—is never a legitimate solution of the original problem. [To put it another way, there is no sum of $M_{-\kappa,\frac{1}{2}}(-x/\kappa)$ and $W_{-\kappa,\frac{1}{2}}(-x/\kappa)$ which can satisfy both boundary conditions (1.2) with κ and λ real.] It is therefore exceedingly dangerous to infer the behavior of the integrated solution from that of a single continuum mode, and this has led to some confusion. For example, Dickinson proved that the momentum flux ($\overline{u'v'}$ in meteorological parlance) is everywhere constant except for a jump at the singularity, and is therefore nonzero on at least one boundary for a *single* continuum mode. Physically, however, this quantity must vary with latitude so as to vanish (like the wave itself) on *both* boundaries. Although this variability has been described[6] as "contrary to a conclusion of Dickinson," such criticism is a comparison of apples and oranges. When the λ integration is performed, mutual cancellation of different values of λ permits $\overline{u'v'}$ to vary and the integrated wave to satisfy the boundary conditions. Since the λ integration cannot be performed analytically, however, this need for integration limits the amount of insight that can be obtained from the continuum modes.

With friction, as in (2.7), be it ever so small, the continuum spectrum breaks up into discrete normal modes which have well-defined limits as the friction tends to zero. The two advantages of this second approach are first, each mode is an independent solution of the original problem so that no integration over λ is necessary. Second, numerical calculations normally incorporate weak dissipation to survive the singularity, so discrete normal modes are what the computer programs actually calculate as in Simmons[7] and Boyd.[9] The disadvantages are that now both the eigenvalues and eigenfunctions are complex and one must wrestle with Stokes' phenomenon.

If no additional approximations or assumptions are made, both approaches—in spite of their great dissimilarity in form—give the same numerical answer. Dickinson (private communication) has suggested a more familiar example that makes this numerical equality more plausible. The Fourier integral

$$I(x) = \int_{-\infty}^{\infty} \frac{e^{i\lambda x}\, d\lambda}{\cosh(\lambda x)} \tag{B1}$$

can be numerically evaluated by direct integration along the real λ axis via the trapezoidal rule. Alternatively, one can complete the contour via a semicircle of infinite radius in the upper half-plane and evaluate the integral as an infinite sum of the residues at the poles of the integrand on the positive imaginary λ axis. These two options are the same as for the singular eigenproblem: the *integral* over *real* λ or the infinite *sum* of discrete *complex* values of λ, and both give the same result.

This point, too, has caused confusion. Physically, verti-

TABLE V. The coefficients of the Chebyshev series for $B\lambda_n$ for the lowest three eigenvalues with $A = -\infty$. The argument of the polynomials is $x = 2^{5/3}/B^{1/3} - 1$. The approximations are accurate for $B \in [4, \infty]$.

Degree of Polynomial	*Mode Number* $n=1$		$n=2$		$n=3$	
	Real part	Imag. part	Real part	Imag. part	Real part	Imag. part
0	1.881 41	1.867 98	−0.444 47	3.436 86	−5.638 86	4.006 26
1	−.237 46	1.011 37	−2.067 50	1.769 41	−6.114 44	1.767 83
2	−.197 85	0.060 24	−0.989 17	−0.063 30	−2.806 82	−0.507 14
3	−.019 13	−0.019 37	−0.152 78	−0.130 97	−0.567 80	−0.273 23
4	0.000 41	−0.002 26	−0.010 63	−0.015 90	−0.053 98	0.022 34
5	0.000 60	−0.000 15	−0.001 99	0.001 28	0.006 91	0.030 18

cally propagating waves must decay exponentially with height because of absorption at the latitude of the singularity. In the discrete modes procedure, the decay rate is dependent upon the imaginary part of λ_n. This might seem worrisome because Dickinson's formalism involves only real λ, but in fact his λ integrated solution[3] decays with height as it should.

Nonetheless, it is obviously desirable to incorporate this decay rate and other properties explicitly in the modes rather than in a λ integration which cannot be analytically performed. For this reason, the discrete modes approach has been adopted here. Because of its greater complexity (literally and figuratively), this procedure is complementary rather than competitive with the continuum modes approach of Dickinson[3] and others.

APPENDIX C: CHEBYSHEV EXPANSIONS FOR THE EIGENVALUES

Although the eigenvalue relation—even when simplified via the WKB method—cannot be solved in terms of any known transcendental, it is nonetheless possible to provide *analytic exact* solutions in the form of Chebyshev series in the parameters. The method is thoroughly explained in Boyd,[22] so it will not be repeated here. To provide a springboard for future work and a sample of the usefulness of the Chebyshev technique, Table V gives the first six expansion coefficients for the lowest three modes with $A = -\infty$.

The form of the approximation is

$$\lambda_n(B) = \frac{1}{B}\left(\frac{1}{2}a_0^{(n)} + \sum_{m=1}^{5} a_m^{(n)} T_m(x)\right), \tag{C1}$$

where

$$x = 2^{5/3}/B^{1/3} - 1. \tag{C2}$$

On the interval $B \in [4, \infty]$, the error in (C1) is at most one part in 4000 for $n = 1$, one part in 700 for $n = 2$, and one part in 200 for $n = 3$.

One can equally well obtain expansions accurate for small B. Accuracy for a given number of polynomials can be improved by choosing a meeting point between the large and small B approximations which increases with n, instead of taking $B = 4$ as the lower limit for all n as done here.

[1]The myth that as in a normal SL problem all the eigenvalues were of one sign persisted until about 1965, when it was discovered that there was in fact an infinite number of eigenvalues of the opposite sign. The eigenfunctions themselves fall into two classes: one class which is oscillatory between the apparent singularities and exponentially small at higher latitudes, and a second class which is oscillatory between the poles and apparent singularities and exponentially small near the equator. Because half the spectrum was left out, all atmospheric tidal calculations up to 1965 were completely wrong. Even then, doubts persisted about the completeness of the eigenfunctions that were not resolved until a rigorous completeness proof was given in 1970. The whole sordid mess is reviewed by R. S. Lindzen, Lect. Appl. Math. **14**, 293–362 (1971).
This history of confusion and error in such recent times for a relatively easy problem should convince the reader that the subject of the present work is far from trivial; because the eigenfunctions are analytic and the eigenvalues are real, an SL problem of the third kind like the tidal equation is much closer to normal SL problems of the first two classes than the singular fourth kind studied here.

[2]A compact and highly readable treatment of normal Sturm–Liouville theory is given in Chap. 6 of P. M. Morse and H. Feshbach, *Methods of Theoretical Physics* (McGraw-Hill, New York, 1953).

[3]R. E. Dickinson, J. Atmos. Sci. **25**, 984 (1968).

[4]K. K. Tung, "Stationary Atmospheric Long Waves and the Phenomena of Blocking and Sudden Warming," Ph. D. Thesis, Harvard University, 1977.

[5]K. K. Tung, Mon. Weather Rev. **107**, 751 (1979).

[6]A. J. Simmons, Q. J. Roy. Meteorol. Soc. **100**, 76 (1974).

[7]A. J. Simmons, Q. J. Roy. Meteorol. Soc. **104**, 595 (1978).

[8]J. P. Boyd, "Planetary Waves and the Semiannual Warming in the tropical Upper Stratosphere," Ph. D. Thesis, Harvard University, 1976; J. P. Boyd, J. Atmos. Sci., to be published (1981).

[9]G. F. Carrier, M. Krook, and C. E. Pearson, *Functions of a Complex Variable* (McGraw-Hill, New York, 1966), p. 319.

[10]An attempt was made to obtain an explicit approximation to λ_{im}, but the lowest order result [to $O(\kappa)$], obtained via the algebraic manipulation language REDUCE2, contained no fewer than 37 terms—too many to be practical. The difficulty is too many parameters: A, B, $\ln(A)$, $\ln(B)$, κ, $\ln(\kappa)$, π, and Euler's constant γ all appear in the equation $\Delta(\kappa) = 0$. [The logarithms come from the $y^{\pm\kappa}$ terms in (4.1) and (4.2).] There is little one can do to simplify the mess because the terms are oscillatory. It can be seen in Table IV that the imaginary part of λ in fact fluctuates irregularly from mode to mode.

[11]J. Heading, *An Introduction to Phase-Integral Methods* (Wiley, New York, 1962).

[12]R. B. Dingle, *Asymptotic Expansions: Their Derivation and Interpretation* (Academic, New York, 1973).

[13]F. W. J. Olver, *Asymptotics and Special Functions* (Academic, New York, 1973).

[14]C. E. Bender and S. A. Orszag, *Advanced Mathematical Methods for Scientists and Engineers* (McGraw-Hill, New York, 1978).

[15]A. H. Nayfeh, *Perturbation Methods* (Wiley, New York, 1973).

[16]There is much confusion in the literature about these definitions. Bender and Orszag (Ref. 14) reverse the terminology without even noting that there is a controversy. The definitions (6.8) and (6.9) are in accord with Stokes' own as discussed in F. W. J. Olver (Ref. 13, p. 518) and also agree with those of J. Heading (Ref. 11) and R. B. Dingle (Ref. 12).

[17]I use the word "convention" because under Poincaré's rather forgiving definition of asymptoticity, any way of varying b across the sector is legitimate so long as $b(A_1)$ and $b(A_2)$ take their proper values. One could, for example, vary b linearly with arg$x$. However, $W_{\kappa,\frac{1}{2}}(y)$ has an exact integral representation, valid for $0 \leqslant \arg y \leqslant \pi$, which upon expansion gives $W_1(x)$ alone as its first term. Though one cannot be entirely comfortable with jumps in the representations of functions which may themselves be smooth or even entire, varying b linearly with arg$y$ or otherwise using a convention different from Stokes' will generally only make the numerical error greater.

[18]Strictly speaking, (6.21) gives the large n asymptotic approximation to the roofs of Ai$(-z)$ rather than the exact zeros, but since the error is only one part in 200 even for $n = 1$, I have ignored this largely irrelevant distinction in the body of the paper.

[19]F. W. J. Olver, Philos. Trans. R. Soc. London, Ser. A **289**, 501 (1978).

[20]M. Abramowitz and I. Stegun, *Handbook of Mathematical Functions* (Dover, New York, 1965), pp. 80–81.

[21]C. W. Lucas, Jr. and C. W. Terril, Commun. ACM **14**, 48 (1971).

[22]J. P. Boyd, J. Math. Phys. **19**, 1445 (1978).